

AD-A136 281

RESEARCH AND CRYSTAL GROWTH ON HIGH DIELECTRIC CONSTANT 1/1  
MATERIALS FOR MM..(U) STANFORD UNIV CA CENTER FOR  
MATERIALS RESEARCH R S FIEGELSON ET AL. NOV 83

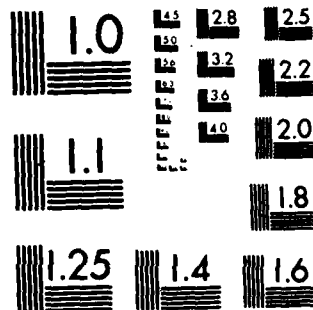
UNCLASSIFIED

CMR-83-11 N00014-82-K-0266

F/G 20/12 NL



END  
DATE  
FILMED  
1 - 84  
DTIC



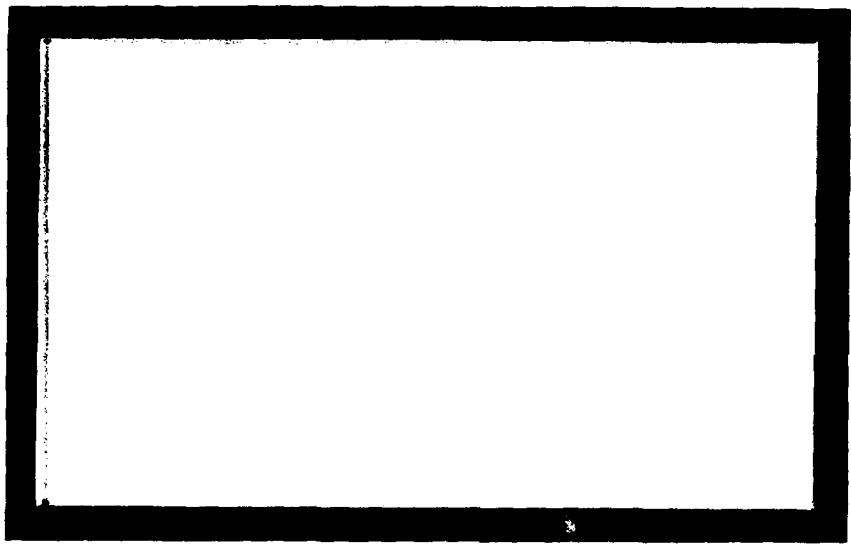
MICROCOPY RESOLUTION TEST CHART  
NATIONAL BUREAU OF STANDARDS 1963-A



12



A136281



DTIC FILE COPY

DTIC  
ELECTE  
DEC 23 1983  
S D D

CENTER FOR MATERIALS RESEARCH

STANFORD UNIVERSITY • STANFORD, CALIFORNIA

DISTRIBUTION STATEMENT A  
Approved for public release;  
Distribution Unlimited

83 12 01 005

12

Accession For	
NTIS GRA&I	<input checked="" type="checkbox"/>
DTIC TAB	<input type="checkbox"/>
Unannounced	<input type="checkbox"/>
Justification	
By <i>Per btr. on file</i>	
Distribution/	
Availability Codes	
Dist	Avail and/or Special
A/1	

Center for Materials Research  
 McCullough Building  
 Stanford University  
 Stanford, CA 94305



Semi-Annual Technical Report  
 on  
 RESEARCH AND CRYSTAL GROWTH ON HIGH DIELECTRIC  
 CONSTANT MATERIALS FOR MM WAVE APPLICATIONS

ONR Contract #N00014-82-K-0266

Submitted to  
 Office of Naval Research  
 CMR-83-11 ✓  
 November 1983

Submitted by  
 The Board of Trustees of  
 Leland Stanford Jr. University  
 Stanford, California 94305

DTIC  
 ELECTE  
 DEC 23 1983  
 S D D

Principal Investigator:

Professor R. S. Feigelson  
 Center for Materials Research  
 Department of Materials Science &  
 Engineering

Associate Investigator:

Dr. D. Elwell  
 Center for Materials Research

**DISTRIBUTION STATEMENT A**  
 Approved for public release;  
 Distribution Unlimited

## I. Introduction

The primary objectives of this program are to grow high-quality single crystals of materials which are candidates for electro-optic phase shifters at mm wavebands. The materials initially selected were (a) the ferroelectric fluorides with the tetragonal  $\text{SrAlF}_5$  structure, (b)  $\text{Ba}_x\text{Sr}_{1-x}\text{TiO}_3$  solid solutions, and (c)  $\text{CdIn}_2\text{Te}_4$ . ~~In the case~~ of  $\text{CdIn}_2\text{Te}_4$ , recent contacts with Hughes Research Laboratories and the Rockwell Science Center indicate a reduced interest in this material, and we have not pursued such studies to date.

During the last six months of the program the main emphasis has been on the synthesis and crystal growth of  $\text{PbAlF}_5$ . The Strontium Salt  $\text{SrAlF}_5$  was the first of a new family of ferroelectric fluorides to be discovered by Ravez and co-workers at the University of Bordeaux (1). These materials have a tetragonal structure with spacegroup I4. Dielectric properties were studied by Ravez on polycrystalline discs made by cold pressing and then sintering in a sealed tube. Only  $\text{SrAlF}_5$  was prepared in the form of very small single crystals.  $\text{SrAlF}_5$  appears to be the only member of this family which melts congruently, although it is rather difficult to prepare as large single crystals because of the volatilization of  $\text{AlF}_3$  from the melt. We successfully grew larger crystals of  $\text{SrAlF}_5$  and some measurements were made on this material at the Hughes Research Laboratories.

$\text{Ba}_{1-x}\text{Sr}_x\text{TiO}_3$  solid solutions are well-known ferroelectrics and our aim is to grow more homogeneous crystals (uniform distribution of Sr and Ba ions) than any produced to date by applying low frequency vibrations to the melt during crystal growth.

Finally, we have started a program to grow single crystals of these and other interesting ferroelectric oxides and fluorides in the form of small rods or fibers ( $\approx 50 \mu\text{m}$  to 1 mm in diameter). This is a relatively quick and easy technique for the preparation of a wide variety of materials in single crystal form. We have recently grown by the laser-heated pedestal growth method what we believe to be the first  $\text{BaTiO}_3$  single crystal fibers from a stoichiometric melt.

## II. Experimental Results

### A. SrAlF<sub>5</sub>

We have grown a clear crystal of good optical quality  $\approx 1 \text{ cm}^3$  in size. Dr. Marvin Klein of Hughes Research Laboratories measured a mm waveband dielectric constant of 7 at room temperature, close to the value measured by Ravez et al. at low frequency. The losses at mm wavelengths were low. These results are promising in two respects: the low losses and the apparent constancy of dielectric constant with frequency. However, the low value of dielectric constant means that this material is not very useful for practical devices and so we decided to shift our emphasis to PbAlF<sub>5</sub> which should have a higher dielectric constant.

### B. PbAlF<sub>5</sub>

The literature is confused on the question of which phases exist in the PbF<sub>2</sub>-AlF<sub>3</sub> system. The reported phase diagram is unreliable and initial work suggests metastable equilibrium may be easily induced. PbAlF<sub>5</sub> has turned out to be a very difficult material to grow in single crystal form but its high dielectric constant, as reported by Ravez et al., combined with the possibility of low losses (by analogy with SrAlF<sub>5</sub>) appear to justify an intensive effort. Crystal growth has been mainly pursued by the vertical Bridgman method using a graphite crucible with a fine capillary. Crystal growth experiments have been carried out over the composition range from 50% PbF<sub>2</sub> (molar) to 73% PbF<sub>2</sub>. The samples are first synthesized from the constituent fluorides by melting in a flowing HF/argon atmosphere which should remove traces of moisture. The crystals are grown in an all-graphite system under purified argon, at a normal growth rate of 0.5 mm/hr.

The results of x-ray analysis of the crystals grown are summarized in Table 1. In this table, the tetragonal ferroelectric phase is labeled F, the other phases found being AlF<sub>3</sub>, Pb<sub>9</sub>Al<sub>2</sub>F<sub>24</sub> and PbF<sub>2</sub> (usually the  $\beta$ -form). The best crystal to date was grown from a starting composition of 58% PbF<sub>2</sub>/42% AlF<sub>3</sub> and has clear, transparent regions over the lower half of the boule, although it shows extensive cracking with possibly small precipitates decorating the cracks.

In parallel with these crystal growth experiments we have carried out an extensive series of experiments aimed at clarifying the phase diagram. Ravez and Dunora (2) reported finding three compounds in the  $\text{PbF}_2\text{-AlF}_3$  system:  $\text{PbAlF}_5$ ,  $\text{PbAl}_2\text{F}_8$  and  $\text{Pb}_9\text{Al}_2\text{F}_{24}$ , the two latter melting incongruently. These phases were produced by synthesis below the liquidus temperature for extended periods in sealed gold tubes. Our reconstruction of an approximate phase diagram based on their data is shown in Fig. 1. In contrast, Shore and Wanklyn (3), using samples cooled from the melt, reported only the compound  $\text{Pb}_3\text{Al}_2\text{F}_{12}$  and used the phase diagram shown in Fig. 2. The  $\text{Pb}_3\text{Al}_2\text{F}_{12}$  phase was reported to have a substantially identical x-ray pattern to Ravez's  $\text{PbAlF}_5$ .

Analysis of samples synthesized in our laboratory at  $800^\circ\text{C}$  (Table 2) shows a transition from excess  $\text{AlF}_3$  for a sample with 53 mole %  $\text{PbF}_2$  to one with excess  $\text{PbF}_2$  for 58 mole %  $\text{PbF}_2$ . This data does not agree with either phase diagram. Samples were also synthesized by heating pressed pellets for 24 hours at  $500^\circ\text{C}$  in graphite containers inside graphitized quartz tubes. The analytical data on these samples is listed in Table 3. This data supports the Ravez conclusion, that the ferroelectric phase is  $\text{PbAlF}_5$ . There is, however, some evidence from our other work for the composition  $\text{Pb}_3\text{Al}_2\text{F}_{12}$  also. For example, preliminary electron microprobe analysis of a clear section of Bridgman grown crystal suggested a Pb:Al ratio of 1.5 rather than 1.0. In addition, the density of crystal pieces averaged  $6.59\text{ g/cm}^3$ , fairly close to the  $6.41\text{ g/cm}^3$  reported for  $\text{Pb}_3\text{Al}_2\text{F}_{12}$  by Shore and Wanklyn, and not to the  $5.91\text{ g/cm}^3$  measured by Ravez for  $\text{PbAlF}_5$ .

In summary, it is still not certain that the tetragonal ferroelectric phase is  $\text{PbAlF}_5$  or  $\text{Pb}_3\text{Al}_2\text{F}_{12}$ . It is of course possible that both phases exist, as in the case of  $\text{BaFeF}_{15}$  and  $\text{Ba}_3\text{Fe}_2\text{F}_{12}$  (4) or perhaps one of these phases in the  $\text{PbF}_2\text{-AlF}_3$  system is metastable. These latter phases also have similar x-ray patterns and a tetragonal structure, although it is surprising that Ravez did not check for the  $\text{Pb}_3\text{Al}_2\text{F}_{12}$  phase in his later investigation of the  $\text{PbF}_2\text{-AlF}_3$  system.

Our DTA data is fairly consistent with the Shore and Wanklyn phase diagram (see Fig. 2), so the assumption that one of the two possible tetragonal phases may be metastable and observed only on

cooling from the melt is reasonable. The possibility also exists that one or the other phases is stabilized by traces of an impurity such as oxygen.

We are currently attempting to resolve this difficult situation by careful analysis of a series of samples formed from the melt under flowing HF in a temperature gradient. Samples will also be synthesized at lower temperatures in sealed tubes, which avoid possible errors due to preferential evaporation of one constituent. Weight losses during synthesis are around 2%, the vapor pressure of  $PbF_2$  being higher than that of  $AlF_3$ .

In addition to the vertical Bridgman experiments described above, we have begun experiments using a horizontal Bridgman method. Evaporation is more severe in this case, but problems due to density differences between the solid and the liquid phase are minimized. We presume that the  $AlF_3$  found at the top of some vertical Bridgman crystals (see Table 1) forms first during solidification but floats to the top of the sample because of its low density. The presence of  $AlF_3$  crystallites could interfere with movement of a stable solid-liquid interface during growth of the tetragonal phase, especially if there is significant convection, and horizontal growth may give improved results. The first such experiment produced a crystal with a translucent section and a very cloudy region, the two regions being of similar composition. Microprobe analysis of this sample is in progress.

#### C. (Ba, Sr) $TiO_3$

System problems described in our last report have been solved. We have now ordered, and expect delivery soon, a specially designed platinum "cold-finger" to hold the seed crystal and to increase the temperature gradient at the crystal-melt interface. The seed crystal will be cooled by a controlled flow of air through a pair of concentric tubes.

Studies of the two novel stirring actions we propose to use for this investigation have been strongly pursued in parallel programs, leading to an improved understanding of the stirring mechanisms.



These stirring techniques will be applied to  $Ba_{1-x}Sr_xTiO_3$  crystal growth as soon as good quality crystals have been grown in the absence of stirring.

#### D. Titanate Fibers

We have grown single crystal fibers of  $BaTiO_3$ , which are probably the first samples of this kind. The fibers were grown from hot-pressed Cerac source material by the laser-heated pedestal method which has been used for a wide variety of materials (5). Fig. 3 is a photograph of a section of a  $BaTiO_3$  fiber.

The high-temperature form of  $BaTiO_3$  is hexagonal, and transforms at  $1460^\circ C$  to the cubic phase which is stable down to the Curie temperature ( $\approx 130^\circ C$ ) where it becomes tetragonal. Cubic crystals are normally grown from a  $TiO_2$ -rich melt so that the hexagonal-cubic transformation can be avoided since it normally leads to severe stresses.

Our first fibers were found to have the high temperature hexagonal form, presumably because of the very high cooling rate which is usual in our fiber growth method. These may be the first single crystals of the hexagonal form of  $BaTiO_3$  produced from stoichiometric melts in a controlled manner and are therefore of academic interest, but the hexagonal phase is not ferroelectric. A cubic  $BaTiO_3$  fiber was grown recently from a  $TiO_2$  rich molten zone, and this approach will be pursued.

We are planning to grow  $Ba_{1-x}Sr_xTiO_3$  single crystal fibers from  $TiO_2$  solutions using our own hot-pressed source material, where the hexagonal phase can in principle then be avoided. It will be of interest to compare the properties of the fiber crystals with bulk crystals grown using top-seeding with vibrational stirring. Fiber crystals should have higher crystalline perfection than bulk crystal and may possess novel properties.

### III. References

1. J. Ravez, S. C. Abrahams, J. P. Chaminade, A. Simon, J. Grannec, and P. Hagenmuller, *Ferroelectrics* 38 (1981) 773; S. C. Abrahams et al. *J. Appl. Phys.* 52 (1981) 4740.
2. J. Ravez and P. Dunora, *C. R. Acad. Sci.* 269 (1969) 331.
3. R. E. Shore and B. M. Wanklyn, *J. Am. Ceram. Soc.* 52 (1969) 79.
4. J. Ravez, J. Viollet, R. de Pape & P. Hagenmuller, *Bull. Soc. Chem. France* 4 (1967) 1325.
5. R. S. Feigelson, *Proc. 6th International School on Crystal Growth, Davos, Switzerland, 1983 (to be published).*

Table 1: PHASES FOUND IN BRIDGMAN CRYSTALS

Mole % $PbF_2$ :	50	53	58	60	62	67	70	73
<u>Region of Crystals:</u>								
End	F+AlF <sub>3</sub>	F+AlF <sub>3</sub>	F+AlF <sub>3</sub>	F+AlF <sub>3</sub>	F+AlF <sub>3</sub>	F+Pb <sub>9</sub> Al <sub>2</sub>	F+Pb <sub>9</sub> Al <sub>2</sub>	F+βPbF <sub>2</sub>
Middle	F+Pb <sub>9</sub> Al <sub>2</sub>	F+AlF <sub>3</sub> (?)	F+Pb <sub>9</sub> Al <sub>2</sub>	F+βPbF <sub>2</sub>	F+Pb <sub>9</sub> Al <sub>2</sub>	F+Pb <sub>9</sub> Al <sub>2</sub>	F+Pb <sub>9</sub> Al <sub>2</sub>	F+Pb <sub>9</sub> Al <sub>2</sub>
One-Third	F+Pb <sub>9</sub> Al <sub>2</sub>	F	F	F+Pb <sub>9</sub> Al <sub>2</sub>	F	F+Pb <sub>9</sub> Al <sub>2</sub>	F+Pb <sub>9</sub> Al <sub>2</sub>	F+Pb <sub>9</sub> Al <sub>2</sub>
Initial	F	F	F	F+Pb <sub>9</sub> Al <sub>2</sub>	F			F+Pb <sub>9</sub> Al <sub>2</sub>

Phases: F = Pb<sub>3</sub>Al<sub>2</sub>F<sub>12</sub> or PbAlF<sub>5</sub> (ferroelectric phase)

Pb<sub>9</sub>Al<sub>2</sub> = Pb<sub>9</sub>Al<sub>2</sub>F<sub>24</sub>

Table 2: X-RAY ANALYSIS OF SAMPLES SYNTHESIZED  
IN HF AT 800°C

Mole % PbF <sub>2</sub> :	50	53	58	60	62	67
Phases Found:	F+AlF <sub>3</sub>	F+AlF <sub>3</sub>	F+PbF <sub>2</sub>	F+PbF <sub>2</sub>	F+PbF <sub>2</sub>	F+PbF <sub>2</sub>

(F = Pb<sub>3</sub>Al<sub>2</sub>F<sub>12</sub> or PbAlF<sub>5</sub>)

Table 3: X-RAY ANALYSIS OF SAMPLES SYNTHESIZED  
AT 500°C IN A SEALED TUBE

Mole % PbF <sub>2</sub> :	40	46	50	56	60
Phases Found:	F+AlF <sub>3</sub>	F+AlF <sub>3</sub>	F	F+Pb <sub>9</sub> Al <sub>2</sub>	F+Pb <sub>9</sub> Al <sub>2</sub>

(F = PbAlF<sub>5</sub> or Pb<sub>3</sub>AlF<sub>12</sub>      Pb<sub>9</sub>Al<sub>2</sub> = Pb<sub>9</sub>Al<sub>2</sub>F<sub>24</sub>)

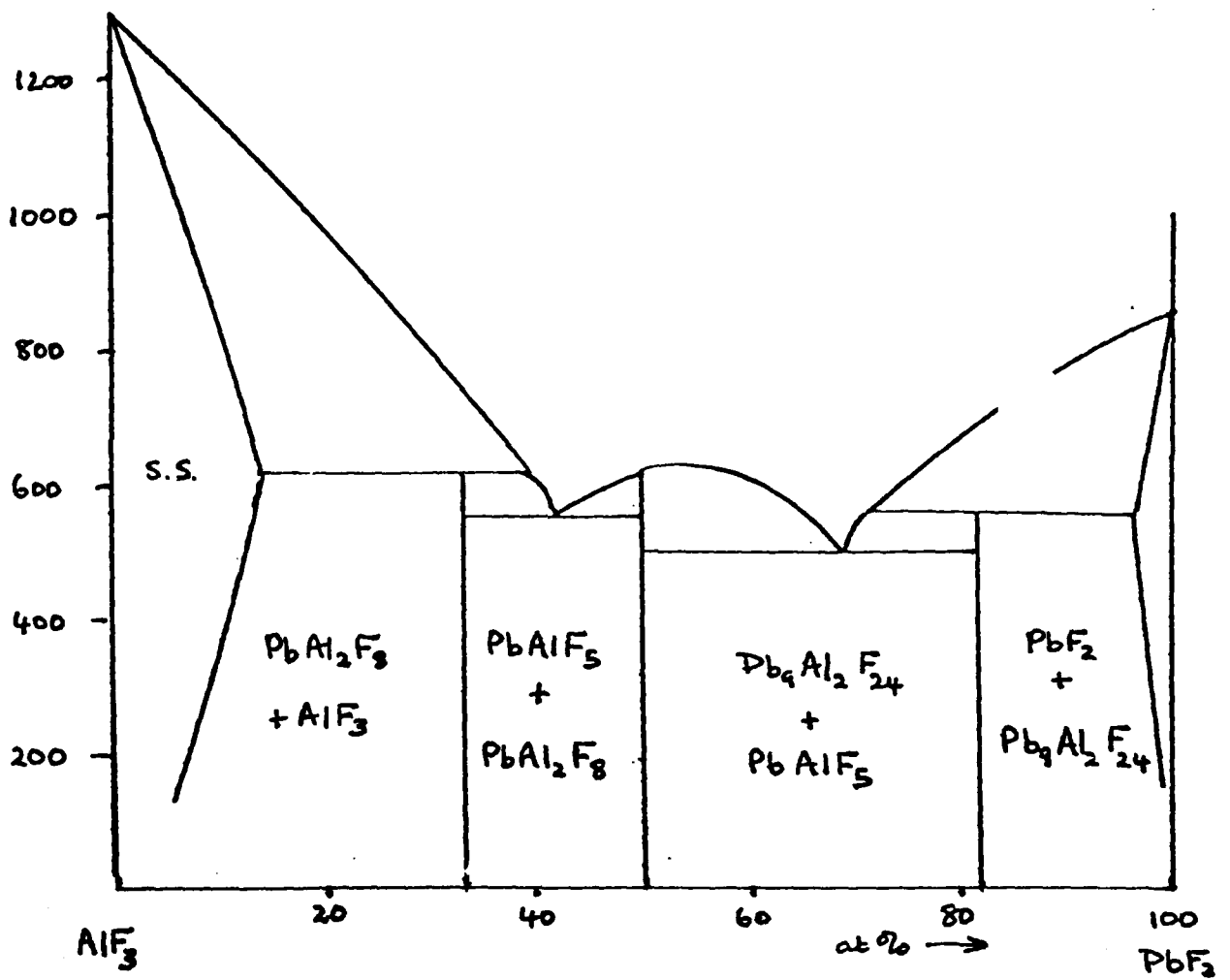


Fig. 1 Approximate phase diagram for  $\text{AlF}_3/\text{PbF}_2$  constructed from the data of Ravez and Dumora (3).

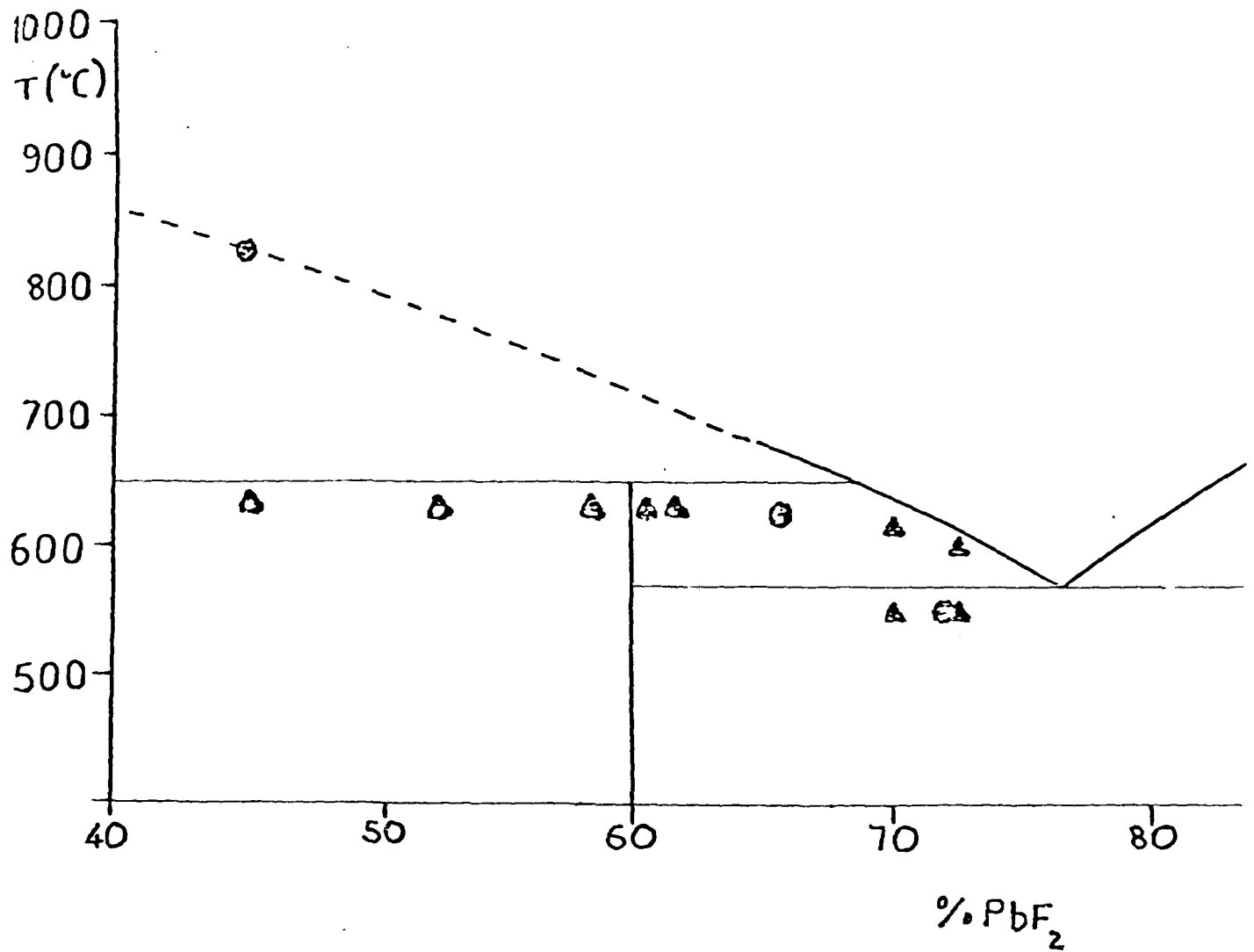


Fig. 2 Phase diagram for the system PbF<sub>2</sub>-AlF<sub>3</sub>: Lines—data from Shore and Wanklyn (4);  $\Delta$  data from DTA heating curves;  $\bullet$  data from DTA cooling curves.

BaTiO

Fig. 3 Section of BaTiO<sub>3</sub> fiber.

